Energy, Mines and Resources Canada
Énergie, Mines et Ressources Canada

CANMET

Canada Centre for Mineral and Energy Technology
Centre canadien de la technologie des minéraux et de l'énergie

Mining Research Laboratories
Laboratoires de recherche minière

ROCK STRESSES AND ROCK STRESS MONITORING IN CANADA

G. Herget

MRL 90-011(TR) *December 1990*

Canada

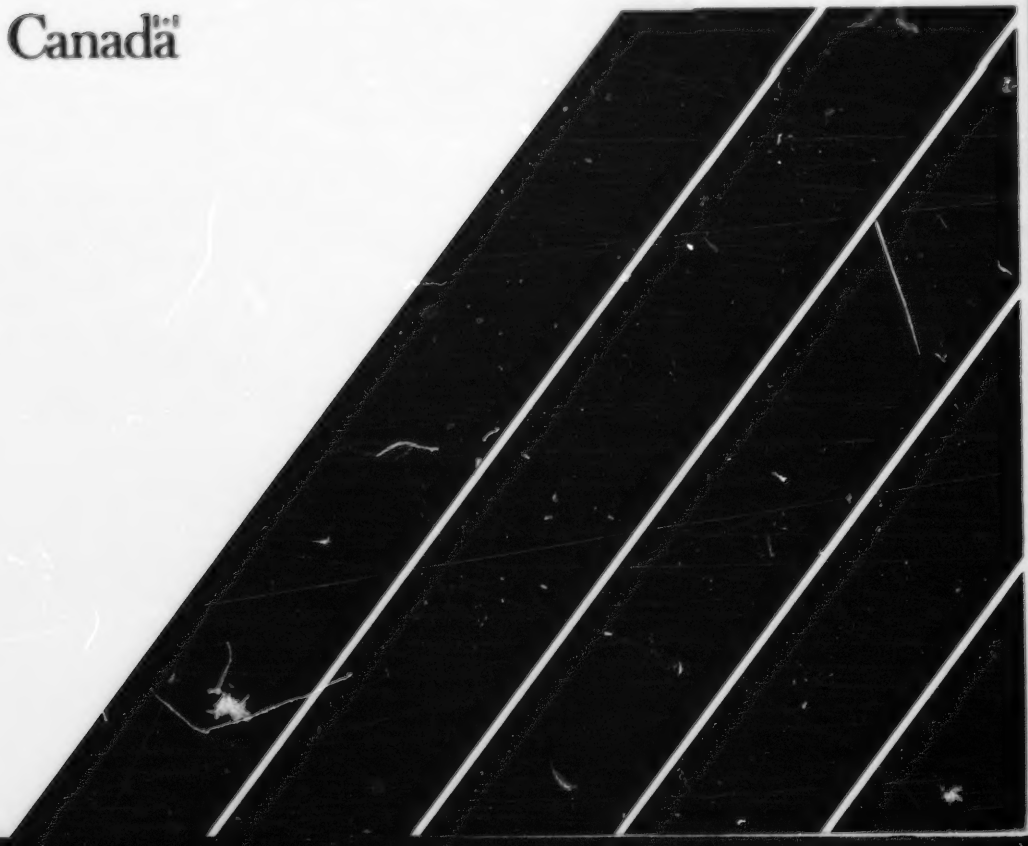

91-04574/

ROCK STRESSES AND ROCK STRESS MONITORING IN CANADA

G. Herget

MRL 90-011(TR) December 1990

53 pp

MICROMEDIA

ROCK STRESSES AND ROCK STRESS MONITORING IN CANADA

G. Herget*

ABSTRACT

A knowledge of rock stresses is essential to establish load assumptions for wall, roof, and floor strata in underground excavation design. Without this information, failure theories and numerical modelling will provide the designer with only qualitative guidance.

Overcoring methods provide the most quantitative ground stress determinations but require very delicate measurements in an adverse environment. The procedures are prone to failure due to debonding of strain gauges, failure of drill core during overcoring and dependence on analytical approaches not matching actual stress/strain behaviour of rock. Quality control is, therefore, of importance. Other stress determination methods can provide essential data where overcoring methods are not suitable, such as in cases where ground stresses exceed the elastic limit of the rock material.

Perseverance and favourable conditions are required to obtain a meaningful on site data base. Many construction projects

---

* Research Scientist, Canadian Mine Technology Laboratory, Mining Research Laboratories CANMET, Energy, Mines and Resources Canada, Ottawa, Ontario

Keywords: Ground stresses, rock mechanics, stress monitoring

do not provide such conditions. It is therefore necessary that quality stress determinations from a number of sites be compiled and analyzed according to general trends and broad geological categories to provide the data base for future projects. Results from the Canadian shield are presented to identify changes of stress magnitudes with depth and regional variations of stress directions.

For the presently available sample of 165 stress tensors the following trends were found (stress magnitudes [MPa], depth [m]):

$$\sigma_1 = 0.0401 \times \text{depth} + 12.25$$

$$\sigma_2 = 0.0292 \times \text{depth} \quad 6.49$$

$$\sigma_3 = 0.0225 \times \text{depth} + 1.41$$

$$\sigma_1/\sigma_v = 297/\text{depth} + 1.8$$

$$\sigma_2/\sigma_v = 155/\text{depth} + 1.3$$

$$\sigma_3/\sigma_v = 341/\text{depth} + 0.9$$

Prevailing directions of principal stresses are σ_1 = NE to E/horizontal, σ_2 = NW to W/horizontal, σ_3 = vertical with large local variations.

Excavations for civil engineering projects and mining operations involve large volumes of rock and ground stresses will vary within these volumes.

Taking this into account and the complexity of inputs which have to be considered in a functional design, it is imperative that ground reaction be monitored at selected points during and after construction to confirm predicted stress redistributions.

Monitoring of mining induced stresses in hardrock with commonly used instrumentation is difficult because of low sensitivity and the minute deformations resulting from stress changes. Recently a number of new borehole devices have been tested in Canadian mines, which allow reliable monitoring of mining induced deformations in the elastic range of hard rock.

SURVEILLANCE DES CONTRAINTES DANS LES ROCHES AU CANADA

G. Herget*

RÉSUMÉ

La conception des excavations souterraines exige de connaître les contraintes qui s'exercent sur les roches pour établir les charges que supportent les couches du toit, du mur et de la sole. Sans ces informations, les théories sur les ruptures et la modélisation numérique ne peuvent fournir au concepteur que des données d'orientation qualitatives.

Les méthodes de surcarottage permettent de déterminer quantitativement les contraintes, mais elles nécessitent des mesures délicates lorsque les conditions ne sont pas favorables. Elles risquent de ne pas être fragmentation de la carotte de sondage durant le surcarottage et de l'obligation de recouvrir à des méthodes analytiques n'établissant pas de corrélation entre le comportement réel sous contrainte et sous déformation de la roche.

---

* Chercheur scientifique, Laboratoire canadien de technologie minière, Laboratoires de recherche minière, CANMET, Énergie, Mines et Ressources Canada, Ottawa (Ontario)

Mots clés: Contraintes dans le sol, mécaniques des roches, surveillance des contraintes

C'est pourquoi le contrôle de la qualité est important. D'autres méthodes de détermination des contraintes peuvent fournir des données essentielles lorsque les méthodes de surcarottage ne sont pas appropriées, lorsque par exemple les contraintes dépassent la limite élastique de la roche.

Pour produire une base de données sur le terrain représentative, il faut être persévérant et pouvoir compter sur des conditions favorables. De nombreux projets de construction n'offrent pas de telles conditions. Il est, par conséquent, nécessaire que les données de qualité sur les contraintes recueillies à de nombreux sites soient compilées et analysées en fonction des tendances générales et des grandes catégories géologiques afin de mettre sur pied la base de données des projets futurs. Les données recueillies dans le bouclier canadien sont présentées pour déterminer les variations de l'amplitude des contraintes en fonction de la profondeur et les variations régionales des directions des contraintes.

Pour les 165 tenseurs de contraintes actuellement disponibles, on a dégagé les tendances suivantes (amplitude de contraintes (MPa), profondeur (m)):

$$\sigma_1 = 0.0401 \times \text{profondeur} + 12.25$$
$$\sigma_2 = 0.0292 \times \text{profondeur} + 6.49$$
$$\sigma_3 = 0.0225 \times \text{profondeur} + 1.41$$
$$\sigma_1/\sigma_v = 297/\text{profondeur} + 1.8$$
$$\sigma_2/\sigma_v = 155/\text{profondeur} + 1.3$$
$$\sigma_3/\sigma_v = 341/\text{profondeur} + 0.9$$

Les directions dominantes des contraintes principales sont $\sigma 1$ = NE à E/horizontal, $\sigma 2$ = NW à W/horizontal, $\sigma 3$ = vertical avec variations locales.

Les excavations réalisées dans le cadre de travaux de génie civil et d'exploitation minière s'appliquent à de grandes quantités de roches, et les contraintes qui s'y exercent varient.

En tenant compte de ce qui précède et de la complexité des données à considérer pour une conception fonctionnelle, il est essentiel que la réaction des terrains soit surveillée à certains points choisis pendant et après la construction pour confirmer les redistributions de contraintes prévues.

La surveillance des contraintes provoquées par l'exploitation minière en roche dure au moyen d'instruments courants est complexe étant donné leur faible sensibilité et les déformations minuscules causées par les modifications des contraintes. Récemment, on a testé de nouveaux appareils de sondage dans des mines canadienne de façon à permettre une surveillance sûre des déformations provoquées par l'exploitation minière dans les roches dures présentant une certaine élasticité.

TABLE OF CONTENTS

	Page
ABSTRACT	i
RESUME	iv
1. INTRODUCTION	1
2. THE CHALLENGE OF SAMPLING	2
2.1 Strategic Locations	3
2.2 Stress Determination Methods	4
2.3 Ground Stresses Below Elastic Limit of Rock	4
2.4 Ground Stresses at Elastic Limit of Rock	5
2.5 Ground Stresses in Excess of the Elastic Limit of Rock	5
2.6 Analytical Models	7
3. STRESSES IN THE CANADIAN LAND MASS	8
3.1 The Canadian Shield	8
3.1.1 Orientation of Principal Stresses	11
3.1.2 Increase of First Stress Invariant with Depth	11
3.1.3 Increase of Principal Stresses with Depth	12
3.1.4 Overburden Load	14
3.1.5 Principal Stress/Vertical Stress Ratios with Depth	15
3.1.6 The Friction Model	16
4. MONITORING OF STRESS CHANGES DURING EXCAVATION ACTIVITY	18
4.1 The CANMET Strain Monitor for Hard Rock	18
4.1.1 Installation and Retrieval	21
4.1.2 Readout and Datalogging	23

TABLE OF CONTENTS (Cont'd)

Page

4.1.3 Calculation of Strains and Stresses from Borehole Diameter Changes 23

4.1.4 Case History: Niobec Mine 27

4.2 Monitoring of Soft Rock 29

5. ACKNOWLEDGEMENTS 31

6. REFERENCES 31

LIST OF FIGURES

No.

2.1 Generalized NW-SE section of Canadian Shield geology at Underground Research Laboratory (URL) site, AECL, Pinawa, Manitoba after [1] 34

2.2 Variation of maximum horizontal stress orientation and magnitude with depth at URL site [1] 34

2.3 Formation of V-shaped notch during URL shaft failure at 277.5-m depth after [1] 35

2.4 Scale effects of in situ stress after [1] 35

2.5 Comparison of principal stress orientations obtained from overcoring in boreholes PH3 and OC2 using closed-form solutions with linear elastic isotropic properties (left) and closed-form solutions with transverse anisotropic linear elastic properties (right) after [1] 35

3.1 Maximum horizontal stress directions in Canada [6] .. 36

3.2 Maximum horizontal stress directions from overcoring in the Canadian shield [13] 36

3.3 Orientation of σ_1 37

3.4 Orientation of σ_2 37

3.5 Orientation of σ_3 37

LIST OF FIGURES (Cont'd)

No.		Page
3.6	Sum of principal stresses with depth	38
3.7	Maximum principal compressive stresses with depth ...	38
3.8	Intermediate principal compressive stresses with depth	38
3.9	Minimum principal compressive stresses with depth	39
3.10	Change of vertical stress with depth	39
3.11	Maximum stress/vertical stress with depth	39
4.1	CANMET single axis strain monitor with hand held readout unit	40
4.2	Calibration curve for CANMET strain monitor	40
4.3	Installation tool for strain monitor	40
4.4	CANMET strain monitor response after production blast	41
4.5	Blasthole open stope at Niobec Mine, Québec	42
4.6	Blasting sequence for C-203-15 and C-203-13 stopes on 850 Level	43
4.7	Response of vibrating wire sensors to blasting activity	43
4.8	Viscosity constant from field data for Saskatchewan potash	44
4.9	CANMET borehole tool establishes deformation rate in potash mine in New Brunswick	44

TABLES

3.1	Statistics of regression of stress magnitudes [MPa] with depth [m]	13
3.1	Analysis of bore hole deformation with modulus of E=57.98 GPa and Poisson's Ration of 0.3	27

1. INTRODUCTION

The assessment of stresses in the rock mass is fundamental in the design of underground excavations. Based on ground stresses, load assumptions can be made for excavation walls, floors and roofs and only then rock strength determinations and computer modelling will allow determination of excavation stability. In addition the determination of stresses for large volumes of rock is of great value for the understanding of geological or geophysical processes ongoing in the earth crust at the present time. This brief overview on stress determinations and stress monitoring in Canada will present some highlights and cannot do justice to all of the work carried out by a number of researchers.

Stresses in rock are a three-dimensional quantity defined by direction and magnitude(tensor). They are a very evasive quantity and are the result of many processes (tectonic, gravity, thermal, etc.) and the physical properties of the rock mass. The paper addresses the problems of obtaining representative ground stress values, the distribution of ground stresses in the Canadian shield and describes recently developed instrumentation for monitoring the effects of load redistribution or stress changes during underground excavation activity.

Terminology, when discussing stresses in rock, can be a problem because of the many processes which effect and alter their magnitude and direction. Geophysicists use a very broad definition of the term "induced" stresses, which encompasses any

alteration of the tectonic stress field due to topography, elastic property changes, local geological structure, erosion and man made effects. Tectonic stresses are typically very uniform over large areas (>10000Km^2) and relate to the magnitude of forces "driving" tectonic plates. Professionals in the engineering field prefer to reserve the term "induced" to describe modifications of the "natural" stress field by man made activities. All stresses discussed here are considered to be free of an induced component in the engineering sense.

2. THE CHALLENGE OF SAMPLING

Stresses are defined as Load/Area(N/m2, MPa, lb/in2) and are derived with Hooke's law by:

Stress = Strain*Elastic modulus

The elastic modulus has the same dimension as stress and is determined on rock samples in the laboratory. Strain is dimensionless and defined as change of deformation over base length. Hooke's law is the basic relationship used for all stress determinations from strain recovery measurements.

Stresses in rock are a very complex quantity. Rock is an assembly of minerals cemented by interstitial matter. Most minerals possess anisotropic mechanical properties and therefore stresses in the rock substance change direction and magnitude from mineral grain to mineral grain. Parts of the solid rock substance are separated by fracture and weakness planes which distort the stress field. In addition the method of stress determination will

introduce its own errors, especially when the elastic limit of the rock is approached.

Most stress determination methods obtain ground stresses for rather small volumes. Designers and geophysicists however, are interested in representative values for rather large volumes of rock. In practise this is difficult to achieve considering the complexity of most geological formations, unless very careful choices are made in regard to the strategic location, stress determination method and analysis prior to the commencement of a stress determination program.

2.1 STRATEGIC LOCATIONS

Stress determinations close to excavation boundaries pick up induced stresses. As a rule of thumb for the determination of pre-excavation stresses, stress determination sites should be located at least 1 1/2 diameter away from the excavation boundary. However, it is more important to recognize that stress fields are distorted near changes in rock type (mechanical properties) or near geological weakness and fracture planes. Faults very often act as domain boundaries for rock units with homogeneous stress fields. At domain boundaries large stress variations may occur. An example is given in Figures 2.1. and 2.2 [1]. A detailed measuring program delineated a number of domains with different stress fields and a high variation of ground stress values within the thrust zone. Measurements in a thrust zone are of little value if one is looking for stress tensors representative of a large volume of rock ($1km^3$).

2.2 STRESS DETERMINATION METHODS

An almost confusing variety of ground stress determination methods exists each with its supporters and claims as to performance. The attached list provides some guidance on method selection based on the magnitude of the ground stresses in regard to the elastic range of the rock substance:

2.3 GROUND STRESSES BELOW ELASTIC LIMIT OF ROCK

Relief methods: These methods use strain gauges or other transducers to measure elastic strain recovery of core when detached from surrounding rock strata by overcoring. Stresses are calculated with Hooke's law. Relief methods provide quantitative results with detailed error calculations in three dimensions but require the rock substance to be fine grained and fracture free. The success ratio is rarely better than 50% and typical procedures use the USBM deformation meter, South African or Australian strain cells. Into this group fit also the large scale methods of underexcavation and mine-by with the recording of convergence.

Fracture induction methods, such as hydraulic fracturing and high pressure dilatometery: One principal stress direction should be known before a test of this type. These are the only methods available for long drill holes.

Stress compensation methods, such as slot and flatjack: They are carried out close to an excavation surface and require the knowledge of principal stress directions to analyse the effect of induced stresses near the excavation boundary.

2.4 GROUND STRESSES AT ELASTIC LIMIT OF ROCK

Seismic and micro-seismic activity is triggered during rock failure and records of events provide information on stress orientation and magnitudes.

2.5 GROUND STRESSES IN EXCESS OF THE ELASTIC LIMIT OF ROCK

Study of induced fracture patterns - borehole breakouts, displacements, kinematic analysis: Failure of a borehole wall occurs when tangential stresses exceed the rock strength. Spalling will elongate the bore hole cross-section in the direction of the minimum principal compressive stress. The study of breakouts in vertical drill holes has provided a very simple method to obtain the orientation of the maximum horizontal stress for large areas relatively quickly [2,3,4].

Studies by Bell and Gough [2,3] have shown for many oil wells in Alberta, Canada that a consistent alignment of the elliptical borehole axes exists for $4*10^5$ km. This consistency is found throughout the Devonian-Cretaceous column and does not change with the dip of beds or the type of rock encountered, such as sand stones and carbonate sediments. Based on their studies the Canadian basin joining the Canadian shield on the westside is subjected to a maximum principal compressive stress oriented northeast-southwest. Hydraulic fracturing and steam injection fracturing in Alberta have supported this analysis. Differences in magnitude between principal stresses do not appear to be large with the maximum principal compressive stress reaching a maximum of about 1.2x overburden stress.

Micro-cracking and failure of the shaft wall at the Underground Research Laboratory (AECL, Pinawa, Manitoba) have been analysed on the same basis as borehole breakouts. The deduced principal stress directions are in agreement with the orientation of ground stresses established by other methods as shown in Figure 2.3 [1]. It is interesting to note that the orientation of the maximum principal compressive stress for this site located on the western boundary of the Canadian shield agrees with the orientation obtained from borehole breakouts in oil wells of the adjoining Interior Platform.

Quality control at each step of the ground stress determination process is imperative because minute differences in strain readings, e.g. from poorly bonded strain gauges, will change results dramatically. Redundancy of readings is therefore necessary to calculate error margins or identify outliers.

One often discussed difficulty is the relationship of the volume which is involved during stress determinations in regard to the volume of rock to which the stresses are to be extrapolated. This is not only a question of the number of measurements to cover a volume adequately but addresses the concern that at different scales, different stresses may exist.

Work carried out recently at the Underground Research Laboratory of AECL, Pinawa, Manitoba has contributed to the understanding of this difficulty. C.D. Martin et al. [5] compare the results from stress determinations carried out at the URL site affecting volumes ranging from $0.1m^3$ to $100000m^3$. The volume of rock for each type of test was calculated assuming that the

diameter (D) of the largest hole drilled, influenced a cylinder of rock six diameters in length and three diameters in radius. The results are reproduced in Figure 2.4. This figure shows convincingly that the same mean stress value, expressed here in the form of the first stress invariant (s1+s2+s3), maybe obtained irrespective of the "volume" of the method, solong more stress measurements are made with the "smaller volume" methods. Measurements based on larger "volume" methods show smaller standard deviations. Therefore, stresses at the engineering scale are penetrative and not subject to a scale effect.

2.6 ANALYTICAL MODELS

By drilling a hole and performing tests in it, the stresses are changed. This change has to be considered in the analysis. Anisotropic mechanical properties must be determined in the laboratory if the rock material exhibits these. Sometimes, even the process of overcoring will produce a mechanical anisotropy by microfracture development. Large errors will arise in regard to the determined magnitude and orientation if the analytical model does not take this into account. Figure 2.5 shows an example from the URL site, Pinawa, Manitoba where the analysis of strain recovery measurements analysed by an isotropic model produced errors in maximum principal compressive stress direction of about 45 degrees.

3. STRESSES IN THE CANADIAN LAND MASS

The Canadian land mass may be subdivided geographically into the Shield Area, the Interior Plains, the Cordilleran Region in the west, and the Appalachian Region in the east. These four regions possess very different characteristics in topography and geology.

A compilation of maximum horizontal stress orientations in Canada as compiled by Adams [6] does however not reflect these regional differences. Across Canada the orientation of the maximum horizontal stress appears to be relatively uniform with an orientation between NE to ENE (Figure 3.1). Locally however, large differences arise due to geological structure and topography.

3.1 THE CANADIAN SHIELD

The Canadian shield is rich in mineral resources and metal mines extend to depths below 2000m. It covers an area of about 4.2×10^6 km^2. Ground stresses have been a major concern for many years because of potential excavation failure and rock bursting.

This section provides an update to previously published compilations by Herget [7, 8, 9] of results of stress determinations made by Canadian mining companies, government agencies and consulting groups.

Most of the tensors reported here have been obtained at mining locations in Ontario, Manitoba and Quebec. The sites are located primarily in the Superior and Southern Tectonic Province

of the Canadian Shield, which consist of Archaen and Proterozoic rocks comprising volcanics, metamorphosed sediments and granites. 0The youngest orogenic deformation occurred during the Grenville Orogeny (955 million years ago).

Fortunately the rock material in the Canadian shield is generally very strong and the application of overcoring methods has permitted stress magnitudes to be obtained based on elastic strain recovery up to 130 MPa. The limit for overcoring tests is generally reached when discing of drill cores occurs. At such rock stress magnitudes the possibility exists that full strain recovery is not measured [10]. It has been observed that the doorstopper method has been used successfully in highly stresses ground, whereas methods requiring the overcoring of an 30-50 cm Ex annulus failed because the hollow core cylinder broke before completion of the test.

In most locations where strain recovery was measured during overcoring, redundant strain recovery data were available for each tensor determination, making possible error determinations using the method of least squares. Errors of ± 10-15% for stress components are common. Details of overcoring methods, quality testing to obtain a high degree of reliability and determination of physical parameters are described elsewhere, [11, 12].

The ground stress tensors reported here are considered to be free from the influence of excavation geometry, e.g. they have been taken at locations in boreholes which were at least 1 to 1½ diameter away from the excavation wall.

Figure 3.2 [13] shows the location of stress determination sites and the orientation of the maximaum horizontal stress. Stresses on the local scale are very complex as indicated earlier in Figures 2.1 and 2.2. The Underground Research Laboratory of Atomic Energy of Canada Limited is located in South Eastern Manitoba, Canada about 100 km east of Winnipeg. Ground stress determinations which have been carried out since 1982 now provide a data base with several hundred stress tensors based on different techniques like overcoring, hydraulic fracturing and convergence measurements during mine by. Connected with this work detailed geological mapping and in situ fracture studies have been carried out.

Results clearly indicate the strong dependence of magnitude and direction of stress components on the geological fabric. Especially fracture zones act as domain boundaries by showing sudden changes in magnitude and direction of stress components. This clearly indicates the difficulties of meaningfully extrapolating ground stress magnitudes and direction obtained in a high strength rock substance.

Results from the stress determination program at the Underground Research Laboratory (MRL), AECL, Pinawa Manitoba have been included in this paper. However, to avoid drowning the relatively sparse sample of stress tensors obtained elsewhere in the Canadian shield, only 8 tensors per domain from the URL data base were admitted to the data pool. This added 32 tensors to the 133 tensors from other areas of the Canadian shield. The 165 ground stress tensors reviewed in this paper are listed in

reference [13] with information on rock types, location and source.

3.1.1 Orientation of Principal Stresses

All principal stress directions of the 165 tensors were plotted in the lower hemisphere of an equal area net. Figures 3.3, 3.4 and 3.5 show that the orientation of principal stress directions possess simple maxima. Concentrations are expressed in percent per 1 percent area:

Sigma 1:	225/05	highest concentration: 6%
Sigma 2:	346/05	highest concentration: 3%
Sigma 3:	115/82	highest concentration: 10%

The most uniform plot is that of Sigma 3. The Sigma 1 direction correlates well with a recent compilation of fault plane solutions, borehole breakouts and hydraulic fracturing data. These show for East and Central parts of North America a very uniform stress field with the maximum principal compressive stress horizontal in a NE to ENE direction (Zoback et al. [14]).

3.1.2 Increase of First Stress Invariant with Depth

The sum of principal stresses is invariant and therefore was used as a check of homogeneity for the sample of 165 stress tensors. The sum of principal stresses was subjected to a straight line regression with depth (Figure 3.6) and a correlation of 0.82 was obtained.

A straight line relationship oversimplifies actual local site conditions if changes in lithology, faults and other discontinuities are present. The specific local variation picked up at the various sites contribute greatly to the large scatter. A comparison of the local URL, AECL data base (32 tensors) with the total sample (165 tensors) is of interest. The regression equations for the AECL sub-sample and the total sample are different. While the correlation coefficient is higher, the difference in magnitude for the AECL mean depth of 211 m is only 48.6 MPa - 39.5 MPa = 9.1 MPa = 23%. Comparing regression statistics of the original 133 tensor sample with those of the 165 tensor sample shows a marginal improvement for the larger data base.

3.1.3 Increase of Principal Stresses with Depth

Statistics in Table 3.1 show that there is a continuous increase of principal stresses with depth. Scatter plots of Figures 3.7, 3.8, 3.9 indicate a slight curvature of principal stress magnitudes with depth. Separating for analysis tensors into groups above 1000 m and below 1000 m did not improve statistical parameters.

Table 3.1 Statistics of regression of stress magnitudes [MPa] with depth [m]

Type	Observations	Regression Coefficient	Std. Error	Constant	Std. Error of Estimate	Correlation Coefficient	T-test	Mean Depth	Mean Magnitude
$\sigma_1+\sigma_2+\sigma_3$	165	0.0918	0.0050	20.1569	34.4517	0.82	18.268	676	82.2
$\sigma_1+\sigma_2+\sigma_3$	32	0.2049	0.0096	5.3631	7.5614	0.96	21.362	211	48.6
$\sigma_1+\sigma_2+\sigma_3$	133	0.0944	0.0060	15.9117	37.1153	0.80	15.631	789	90.4
$\sigma 1$	165	0.0403	0.0020	12.1013	13.8865	0.84	19.961		
$\sigma 1$	32	0.1083	0.0057	2.1307	4.4617	0.96	19.137		
$\sigma 1$	133	0.0411	0.0023	10.4445	14.4346	0.83	17.497		
$\sigma 2$	165	0.0293	0.0019	6.4022	12.7724	0.77	15.777		
$\sigma 2$	32	0.0623	0.0040	1.8221	3.1650	0.94	15.514		
$\sigma 2$	133	0.0298	0.0023	5.4663	13.9632	0.75	12.402		
$\sigma 3$	165	0.0225	0.0015	1.3894	10.5942	0.75	14.642		
$\sigma 3$	32	0.0343	0.0036	1.4104	2.8527	0.86	9.478		
$\sigma 3$	133	0.0235	0.0019	0.00927	11.6606	0.73	12.402		
$\sigma 1/\sigma v$[1)]	165	272.3166	8.2169	1.7165	1.3981	0.93	33.141		
$\sigma 2/\sigma v$	165	140.9055	6.2640	1.1837	1.0658	0.87	22.495		
$\sigma 3/\sigma v$	165	30.2982	3.5359	0.8560	0.6016	0.56	8.569		

[1)] σv = 0.0285MPa/m

Therefore a straight line regression of principal stresses over the full depth range was used. The results were as follows:

	Sigma 1	Sigma 2	Sigma 3
Intercept (MPa):	12.25	6.49	1.41
Gradient (MPa/m):	0.0401±0.0020	0.0292±0.0019	0.0225±0.0016
Correlation coefficient:	0.84	0.78	0.75

3.1.4 Overburden Load

Many investigators have observed that the vertical stress component (S_v) increases linearly with depth and that the increase is related to overburden weight. The density for rocks rich in quartz and feldspar is about 2650 kg/m3 and 3300 kg/m^3 for basic and ultrabasic rocks. This results in a vertical stress gradient of 0.0260 to 0.0324 MPa/m depending on the density of the rock formation involved.

Analysis of minimum principal compressive stress orientations in Figure 3.5 indicates that only 10% of the minimum stress components are oriented exactly vertical. The minimum principal compressive stress has a gradient of 0.0225 MPa/m with an intercept of 1.4 MPa. This indicates that the vertical stress gradient from overburden exceeds that of the average minimum principal compressive stress.

For this purpose the vertical stress component was calculated from the principal stressed listed and the regression line was determined to be 0.0285 MPa/m (Figure 3.10).

From observations of seismic activity around large hydro dams and isostatic adjustments due to melting ice sheets, it appears that the earth's crust is maintaining a delicate balance

in the vertical direction and will adjust to changes in vertical loading of 0.5 to 1.0 MPa for large areas [14].

3.1.5 Principal Stress/Vertical Stress Ratios with Depth

Calculation of principal stress/vertical stress ratios were calculated with the average σv gradient and subjected to a regression in relation to the inverse of depth (Fig. 3.11). The following statistics were obtained for the equation:

Ratio = (Regression coefficient/depth (m) + constant

	$\sigma_1/\sigma v$	σ_2/σ	$\sigma_3/\sigma v$
Constant:	1.7	1.25	0.90
Regression coefficient:	272±8	155±6	34±4
Correlation Coefficient:	0.93	0.88	0.57

Hydraulic fracturing provides an alternative method of ground stress determination. In recent years interpretation techniques have been refined considerably with regard to the analysis of time/pressure diagrams. Thirteen values of a recently published hydraulic fracturing experiment in the Easten part of the US are quoted from D.R. Schmitt and M.D. Zoback [16] and

J. Baumgärtner and M.D. Zoback [17] below:

	Depth (m)	Sigma[1] (MPa)	Vert[1] (MPa)	S1/Vert	
1	108	26.6	2.8	9.63	Kent Cliffs,
2	553	37.9	14.1	2.68	Schmitt et al. 1989
3	586	39.7	15.0	2.65	
4	646	53.5	16.5	3.24	
5	108	12.0	2.8	4.34	Moodus Wellbore,
6	117	11.4	3.0	3.81	Baumgärtner et
7	178	24.9	4.6	5.47	al. 1989
8	193	19.9	4.9	4.03	1) density 2.61g/cm^3
9	819	45.2	20.9	2.16	
10	837	14.3	21.4	.67	
11	890	50.6	22.8	2.22	
12	1076	70.5	27.5	2.56	
13	1284	79.9	32.8	2.43	

Calculation of regression σ_1 with depth provided the following regression equation:

$$\sigma_1 = 11.4538\text{MPa} + 0.0456\ \text{MPa/m}$$

with a correlation coefficient of 0.83. This is in good agreement with the results from the Canadian shield.

The ratio σ_1 / σ_v with depth provided the following regression equation:

$$\sigma_1 / \sigma_v = 491/\text{m} + 1.7105$$

with a correlation coefficient of 0.76.

3.1.6 The Friction Model

Ground stresses in the earth crust are very likely at the long-term strength limit of the crust. [18]. A criterion based on shear failure is readily quantified based on the ratio of σ_1/σ_3:

$$(\sigma_1 - Po) / (\sigma_3 - Po) = [(\mu^2 + 1)^{1/2} + \mu]^2$$

where Po = pore pressure, e.g. hydrostatic pressure and μ = coefficient of friction.

This shear failure criterion can be rewritten to define the friction angle:

$$\mu = [R/4 - \tfrac{1}{2} + 1/(4R)]^{\frac{1}{2}},$$

where R = σ_1 / σ_3 ratio.

Using the above equation and the calculated depth dependence of σ_1 / σ_3 the following friction values were obtained:

Depth (m)	Ratio (σ_1/σ_3)	Coefficient of Friction	Angle of Friction
300m (Po = 0)	3.09	0.59	30.7
300m (Po = hydrostatic)	3.51	0.67	33.8
3000m (Po = 0)	1.95	0.12	18.8
3000m (Po = hydrostatic)	2.93	0.56	29.4

The obtained angles of friction are well within the range of laboratory determined shear stress/normal stress ratios for rock surfaces subjected to relatively high normal stresses. As an example values for shear stress/normal stress ratios obtained in laboratory shear tests varied in a rather narrow range e.g. 0.3 to 0.85 [19]. Thus the coefficients of friction of 0.3 and 0.85 may be used to provide upper and lower bounds for the maximum principal compressive stress calculated from the equation linking ground stresses and friction.

4. MONITORING STRESS CHANGES DURING EXCAVATION ACTIVITY

Results from the determination of ground stresses and mechanical properties of large volumes of rock carry many uncertainties. Thus the prediction of load redistribution during excavation activities need to be checked. Load redistribution causes deformation which are very small for hard, high modulus rock in the elastic range. Moisture, dust and blasting demand rugged instrumentation capable to read 0.001 mm reliably. Very valuable information has been obtained with extensometers measuring displacements parallel to drillhole axes. Recently a high resolution borehole diameter monitoring device was developed to record reliably the rather minute elastic rock deformations. The borehole measuring device and ancillary equipment are described in this report. An example of its use is provided by one case history. A similar borehole device for softrock is also described.

4.1 THE CANMET STRAIN MONITOR FOR HARD ROCK

Based on the reliable long-term performance of vibrating wire sensors, a relatively stiff ring was developed at the Mining Research Laboratories of CANMET (Canada Centre for Mineral and Energy Technology) which is set with guided wedges into 76 to 153 mm diameter (2.98 in., 4.66 in., 6 in.) drill holes. In the following sections, the mechanical assembly of the CANMET strain ring is described with the peripheral equip-ment required for installation and data capture [20, 21, 22].

Figure 4.1 shows the CANMET strain monitoring system. It comprises a vibrating wire sensor and a read-out unit. The sensor consists of a steel ring which carries a vibrating wire with exciter unit to read the resonant frequency of the wire. As the steel ring is deformed and the wire in turn is either stretched or shortened, this resonant frequency changes.

Figure 4.2 shows a calibration curve for a vibrating wire sensor built for a 153 mm (6 in.) diameter drill hole. The 0.3 mm (0.012 in.) diameter piano wire has a length of 100 mm (4 in.). As the exciter unit and read-out system are stable to 1 Hz, deformations of 0.0004 mm (0.00001 in.) can be reliably detected. For a borehole with a 153 mm (6 in.) diameter the resolution is 0.00003 strain. The sensor is a deformation monitoring device but with suitable calibration it can be used to monitor load or stresses for specific rock materials.

The vibrating wire is typically made of high strength piano wire which has to be firmly clamped into the proving ring. The clamping mechanism has to be such that clean vibrations are achieved and that no creep occurs at the clamping points. The pull on the piano wire lies typically between 5 to 15 lbs. For the CANMET strain rings a special split tube seat was developed to clamp the wire.

The dimensions of the proving ring were arrived at with a number of closed form solutions and finite element analysis. The intent was to achieve the following:

1. high contact pressures to achieve reliable readings and blast vibration resistance;

2. uniform deformation of sensor when installed, e.g. avoid twisting or misaligning;
3. ring stiffness below rock stiffness;
4. vibrating wire deformation below yield point of piano wire;
5. achieve resolution to monitor elastic deformation in hard rock, e.g. better than 0.0001 mm /Hz;
6. generous dimensions to allow recovery of units after use or allow calibration checks during long monitoring programs;
7. vibrating wire mounted at right angle to loading direction, and
8. stable calibration with dual wedge system.

The most quantitative results were obtained by finite element analysis. For an installation in a 153 mm (6 in.) diameter hole an outside diameter of 127 mm (5 in.) and an inside diameter of 89 mm (3.5 in) was chosen. A hardened steel ring deforms by about 0.38 mm (0.015 in.) under a load of 50 kN (11240 lbs). The seating pressure is about 18 kN (4047 lbs).

This changes the vibrating wire frequency by about 200 Hz. These high seating forces are very beneficial. They achieve firm contact in the drill hole by crushing minor asperities and make the installation resistant to accelerations during blasting.

As can be seen in Figure 4.1, there are two grooves machined into the proving ring which are located on a diameter. The grooves have a taper of about 3° which accept complimentary wedges. During movement of the wedges along the proving ring, the outer surface of the wedges remains parallel to the borehole axis.

These wedges are activated during installation by a hydraulic piston. The installing tool is described in the following Section. High seating pressures and precise guidance for the contact wedges ensure that the rings perform on site as calibrated in the laboratory. The list below describes the dimensions of presently available sensors (dimensions in mm):

Drill hole size	Ring O.D.	Ring I.D.	Hole diameter range	Resolution (mm/Hz)	Sensor Range
153	127	89	149-159	0.0004	0.38
118	99	67	116-126	0.0003	0.25
76	64	43	73-80	0.0002	0.20

The stiffness is about 140MN/m.

The above hole sizes were chosen because of their common use in stress determinations or in geotechnical site investigations.

There is some temperature dependence of the resonant frequency of the vibrating wire sensors as given in Figure 4.3. A total of 284 data pairs of resonant frequency at rest and temperature in °C for a sensor subjected to a temperature change of 0° to 20 °C were read at 15 minute intervals. Figure 3 is for a CANMET hardrock ring made for a 76 mm diameter bore hole. The regression showed a temperature dependency of about 1 Hz per degree C with a correlation coefficient of 0.99.

4.1.1 Installation and Retrieval

The sensors are preferably installed in diamond drilled holes but percussion drilled holes reamed to the required size are also suitable. The installation is carried out with a hydraulic

piston which activates a pushbar and in turn pushes the wedges along the grooves as the steel ring is held firmly in place by two metal arms (Figure 4.3). The metal arms are connected to the ring by countersunk flathead screws. When the required seating pressure is reached, these metal screws are sheared and the ring is disconnected from the installing tool. The installing tool can then be retrieved. The material and the diameter of the attachment screws are chosen on the basis of the seating pressure required for the rings. ¼ - 28 brass screws with drilled out centres have been used successfully.

The mechanical seating of the rings and their generous dimensions allow recovery of the sensors after use. For this purpose, the arms on the installing tool are equipped with a key which is pushed past the wedges of an installed ring and rotated to engage the wedges. By activating the hydraulic pressure pump, the wedges are held while the sensor is pushed off the wedges with the pushbar and a spacer. After the wedges are loose, ring and wedges are retrieved. These sensors can be recalibrated in the laboratory and installed at some other location. If borehole deformation has been small, a long drill steel pushed hard against the ring will drive the ring off the wedges for recovery. This will not be effective if borehole deformation has been severe.

The wedge location on the borehole wall determines the diameter along which the borehole deformation is monitored. The orientation switch is mounted on the installation tool to allow the selection of locations around the borehole wall in 45° increments. An installation of four rings (at 0° (horizontal),

45°, 90° (vertical) and 135° with the angles measured anti-clockwise from horizontal right for an observer looking into the drill hole) provides one redundant reading. This allows calculation of measurement errors and assessment as to the rocks elastic behaviour.

4.1.2 Readout and Datalogging

The oscillator circuit used to vibrate the wire is enclosed within the ring. The power consumption for continuous oscillation is about 20 mA. The read-out unit records frequency and is only slightly larger than a pocket calculator (Figure 4.1).

Commercial data logging units like the Grant Squirrel 1201 (42 k storage capacity) have been used successfully to record vibrating wire sensors in mines for many weeks. However, a waterproof data logger was developed which has four frequency and four thermistor channels. This unit, including the battery power supply is housed in a metal pipe 58 mm (2.25 in.) diameter and 533 mm (21 in.) long. The logger can be completely hidden within the borehole, is waterproof and can be left unattended for 6 months at a time.

The data logger and the vibrating wire sensors have successfully operated in a temperature range of -20° C to + 50° C.

4.1.3 Calculations of Strains and Stresses from Borehole Diameter Changes

Ideally the three-dimensional stress tensor should be determined at each monitoring location. However, for an

with:

U = deformation of borehole diameter

d = borehole diameter

E = elastic modulus

6_1 = maximum principal stress

6_2 = minimum principal stress

θ = angle from horizontal counter clockwise

If a rectangular pattern of sensor orientation is maintained for the CANMET strain monitors, the solution below will provide the magnitude and orientation of principal stresses. The angles below are counted anticlockwise from horizontal right with the observer looking into the drill hole.

As an example, the following strains were obtained after monitoring by applying the calibration factor and dividing by the borehole diameter:

Instrument 1. θ = 0° (horizontal) = $\epsilon 0$ = 0.000310

Instrument 2. θ = 45° (45 degree) = ϵ_{45} = 0.000080

Instrument 3. θ = 90° (vertical) = ϵ_{90} = 0.000050

Maximum principal strain (ϵ_1):

$$\epsilon_1 = 0.5\ (\epsilon_0+\epsilon_{90})+0.5[2(\epsilon_0-\epsilon_{45})^2+2(\epsilon_{45}-\epsilon_{90})^2]^{0.5}$$

$$\epsilon_1 = 0.5\ (310+50)+0.5\ [2(310-80)^2+2(80-50)^2]^{0.5} = \underline{0.000344\epsilon}$$

Minor principal strain (ϵ_2):

$$\epsilon_2 = 0.5\ (\epsilon_0+\epsilon_{90})-0.5[2(\epsilon_0-\epsilon_{45})^2+2(\epsilon_{45}-\epsilon_{90})^2]^{0.5}$$

$$\epsilon_2 = \underline{0.000016\epsilon}$$

The principal strain directions are:

$$\tan 2\theta(\epsilon_1, \epsilon_2) = \frac{\epsilon_{45}-(\epsilon_0 + \epsilon_{90})}{\epsilon_0 - \epsilon_{90}} = \frac{160-360}{260} = -0.769$$

$\arctan(-0.769) = -37.56 = 2\theta$

$\theta = -18.78°$ identifies the direction of one of the principal strains ϵ_1 or ϵ_2. $\theta\epsilon_1$, must make an angle of less than 45° with the algebraically greater normal strain, which in this case is 0.000310ϵ.

Thus the -18.78° identify the direction of the maximum principal compressive strain.

For the elastic isotropic case the directions of principal stresses agree with those of the principal strains.

Maximum principal stress (σ_1):

$$\sigma_1 = \frac{E(\epsilon_1 + R\,\epsilon_2)}{1-R^2}$$

For the above case with elastic modulus (E) = 69 GPa and Poisson's Ratio (R) = 0.25:

$$\sigma_1 = \frac{69\text{GPa}\ (0.000343+0.25 \times 0.000017}{1 - 0.25^2} = \underline{25.6\text{MPa}}$$

Minor principal stress (σ_2):

$$\sigma_2 = \frac{E(\epsilon_2 + R\epsilon_1)}{1 - R^2}$$

$$\sigma_2 = \frac{69GPa\ (0.000017 + 0.25\ x\ 0.000343)}{- 0.25SUP2} = \underline{7.6MPa}$$

If one additional diameter is monitored, e.g. at 135°, it is possible to calculate the strain ellipse 4 times by combining every time a different set of three diameters, e.g.: (123, 124, 234, 341). If the solutions for the four sets agree, then the conditions of elasticity are fulfilled and the monitoring procedure is very precise. If not, then the redundant reading

allows calculation of a solution of best fit and a calculation of error according to the method of least squares.

An example of how measurements of borehole diameter changes may agree is given in Table 4.1 with data from a deep hard rock mine. A production blast (881204) increased the maximum biaxial stress by (2.46 ± 0.06) MPa in a nearly horizontal direction. Figure 4.4 provides the reaction of four CANMET strain monitors to this production blast.

Table 4.1: Analysis of bore hole deformation with a modulus of E = 57.98 GPa and Poisson's Ratio of 0.3.

Strain Directions	Maximum Stress (MPa)	Minimum Stress (MPa)	Angle of Maximum Stress to Horizontal
θ = 90, 135, 0	2.5	- 0.81	- 6.2
θ = 45, 90, 135	2.38	- 0.86	- 7.2
θ = 0, 45, 90	2.52	- 0.83	- 7.8
θ = 135, 0, 45	2.47	- 0.95	- 6.8
	Average 2.46±0.06	- 0.86±0.06	- 7.0±0.7

4.1.4 Case History: Niobec Mine

In July 1986, six CANMET strain monitors were installed at the Niobec mine in 153 mm diameter drillholes which had been previously used for ground stress determinations. The Niobec mine is located about 380 km NNE of Montreal, Quebec. About 1500 tons of ore are produced per day from a trackless blasthole open stoping operation. This mine produces Niobium oxide from a carbonatite body.

The standard pillar width is about 25 m followed by 25 m wide stopes. Stopes are up to 60 m long from hangingwall to footwall and stope height is 100 m (Figure 4.5).

The instrumentation was installed in T-213-13 pillar and in the overcut of C-203-15 stope at 850 level, in drill holes available after overcoring for stress determinations. The sites at 265 m below surface and ring orientations are shown in Figure 4.6. The objective was to see whether stope C-203-15 would produce measurable deformation.

Monitoring at sites 1 to 3 started on July 15, 1986 and continued until sites 2 and 3 disappeared in a production blast. The sensors were recovered before hand. Monitoring at site 1, main pillar (T-212-13), continued until March 1988.

The results are shown in Figure 4.7 with the major events responsible for borehole deformation. The records were of unique quality with the instruments providing consistent responses when blasting changed excavation geometry.

The 153 mm diameter drill hole at site 1 had one vertical and one horizontal ring installed. Both units operated throughout the monitoring period. The most significant response was observed between November 6 and 11, 1986. This showed an increase in the horizontal direction of 2 Hz (=0.0008 mm) across the diameter. This was triggered by blast No. 38 removing 18800 t of ore in T-203-12 stope. This blast was opposite to the ring locations and extended from 1000 to 850 level. It indicated a loss of horizontal confinement at the monitoring site of about 9 MPa based on two dimensional analysis. Loading in the vertical direction

was not shown.

Sites 2 and 3 were located in the overcut of C-203-15 stope. The vibrating wire sensors were installed along the pillar centre line prior to the development of drill drifts on each side for use of production drilling equipment. The most severe reaction was observed between November 26 and December 5, 1986. Rings 1 and 3 which were monitoring in the horizontal direction at site 2 recorded expansions of 134 Hz (0.054 mm) and 124 Hz (=0.05 mm) respectively. The vertical reaction at site 2 was -44 Hz (0.018 mm) closure. Examination of blasting records identified slashes 3 and 4 in the overcut of C-203-15 stope opposite the instrumentation site as the cause. These records show a relaxation of 8.4 MPa in the horizontal direction and a loading of only 0.07 MPa in the vertical direction.

Site 3 sensors monitored the vertical diameter only. Ring 4 indicated no response to slashes 3 and 4 while ring 2 indicated a vertical compression of 24 Hz (=0.01 mm). All rings monitoring the vertical direction showed little load change.

4.2 MONITORING OF SOFT ROCK

Redistribution of loads occurs during any excavation activity. In hard rock it is manifested by stress increases and strain energy storage. Soft rocks like potash, salt and some coals do not have the capability of storing large amounts of strain energy because of their limited elastic range. These types of rock will react with increased flow during the period while loads are being distributed to surrounding strata. Higher

deformations resulting from higher stresses be readily identified by convergence meters and extensometers. At a Saskatchewan potash mine hydraulic pressure cells and extensometers have been used to record stresses and deformations in the walls and roof of excavations as given in table 3.2. This showed that pressures in the walls were much higher than in the roof. The different strain rates could be explained by a uniform viscosity constant as presented in Figure 4.8. Regression provided a field viscosity constant of $0.104*10^6$ day MPa/ϵ. This shows that in viscous rock, measurements of ground stress change may be replaced by determinations of deformation rate. Therefore the measurement of deformation rate may be used as an indicator of excavation loading in soft or viscous rock.

At a potash mine in New Brunswick the rate of deformation has been used successfully to predict longterm excavation performance. For instance the following guide lines have been developed for horizontal closure in main entries (5x12m):

Deformation rate (mm/day)	Condition
less than 0.15	excellent
0.15-0.30	good
more than 0.70	poor

To facilitate the measurement of deformation rates the Mining Research Laboratories of CANMET, EMR have developed a borehole monitoring instrument which connected to in the hole data loggers will provide meaningful deformation rates within a few days. The total range is 2mm and the resolution is 0.002mm. Figure 4.9 shows an example for this device where a constant deformation rate was established within five days.

5. ACKNOWLEDGEMENTS

This compilation is part of a rock mechanics research project carried out at a number of mine sites. The author appreciates very much the good cooperation with mine staff and the effort which was put into site preparation and recording of mining activity.

6. REFERENCES

1. Martin C.D. Characterizing in situ stress domains at AECL's Underground Research Laboratory. Proc. 42nd Cdn. Geot. Conf. Winnipeg (1989).

2. Gough D.I. and J.S. Bell. Stress orientations from oil-well fractures in Alberta and Texas. Can. J. Earth Sci. 18, pp. 638-645 (1981).

3. Bell J.S. and D.I Gough. Northeast-southwest compressive stress in Alberta: Evidence from oil wells. Earth and Planetary Science Letters, 45, pp. 475-482 (1989).

4. Guenot A. Borehole breakouts and stress fields. Int. J. Rock Mech. Min. Sci & Geomech. Abstracts 26-3/4, pp. 185-195 (1989).

5. Martin C.D., R.S. Read., N.A. Chandler. Does scale influence in situ stress measurements? - some findings at the Underground Research Laboratory. Proc. Workshop on Scale Effects, LCEN, Norway (1990). - in print.

6. Adams J. Crustal stresses in eastern Canada. In Earth Quakes at North-Atlantic Passive Margins: Neotectonics and post glacial rebound, (Edited by S. Gregersen and P.W. Bashem), Kluwer Academic Publishers pp. 289-297 (1989).

7. Herget G. Variation of rock stress with depth at a Canadian iron mine. Int. J. Rock Mech. Min. Sci. 10, pp. 37-51 (1973).

8. Herget G. High stress occurrences in the Canadian shield. Issues in rock mechanics. 23rd US Symposium on Rock Mech., Berkeley, pp. 203-210 (1980).

9. Herget G. Changes of ground stresses with depth in the Canadian shield. Proc. Int'l Symp. on Rock Stress and Rock Stress Measurements, Stockholm, pp. 61-68 (1986).

10. Hast N. Limit of stress measurements in the earth's crust. Rock Mechanics, 11, pp. 143-150 (1979).

11. Leeman E.R. The "doorstopper" and triaxial rock stress measuring instruments developed by the CSIR. J. South African Inst. Min. Met., Vol. 69, 99. pp. 305-339 (1969).

12. Gray W.M. and K. Barron. Stress determinations from strain relief measurements on the ends of boreholes; planning, data evaluation and error assessment. Proc. Int. Symp. on Determination of Stress in Rock Masses, Lisbon (1969).

13. Herget G. and B. Arjang. Update on ground stresses in the Canadian shield. Proc. Conf. on Stresses in Underground Structures, CANMET, Ottawa p.p. 33-47 (1990).

14. Artyushkov E.V. Rheological properties of the crust and upper mantel according to data on isostatic movements. Geophysical Research, Vol. 76, No. 5 (1971).

15. Zoback M. Lou, et. al. Global patterns of tectonic stress. Nature, 341, pp. 291-298 (1989).

16. Schmitt D.R. and M.D. Zoback. Poroelastic effects in the determination of the maximum horizontal principal stress in hydraulic fracturing tests - a proposed breakdown equation employing a modified effective stress relation for tensile failures. Int. J. Rock Mech. Min. Sci. & Geom. Abstracts, 26-6, pp. 499-506 (1989).

17. Baumgartner J. and M.D. Zoback. Interpretation of hydraulic fraturing pressure-time records using interactive analysis methods. Int. J. Rock Mech. Min. Sci. & Geom. Abstracts, 26-6, pp. 461-469 (1989).

18. Hast N. The state of stress in the upper part of the earth's crust. Tectonophysics, Vol. 8, pp. 189-221 (1969).

19. Jaeger J.C. The frictional properties of joints in rock. Geofis. pura appl., 43, pp. 148-158 (1959).

20. Herget G. and F. Kapeller. Monitoring equipment for mining induced stresses at Niobec mine. Proc. 5th Int'l Symp on Deformation Surveys and 5th Canadian Symp. on Mining Surveying and Rock Deformation Measurements, pp. 198-207, Fredericton, N.B. (1988).

21. Herget G. and F. Kapeller. CANMET tests strain monitor. Technology Update, World Mining Equipment, pp. 50-54, London (1988).

22. Herget G. CANMET strain monitors for hardrock: description, installation, analysis. MRL 89-119(TR) (1989).

23. Herget G. Stresses in rock, 179 p, A.A. Balkema, Rotterdam (1988).

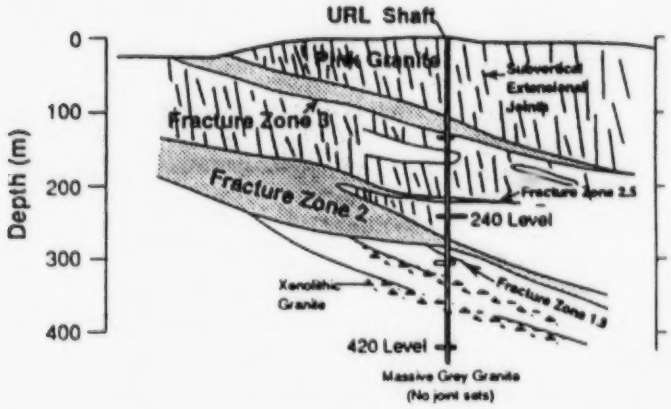

Figure 2.1 Generalized NW-SE section of Canadian Shield geology at Underground Research Laboratory (URL) site, AECL, Pinawa, Manitoba after [1]

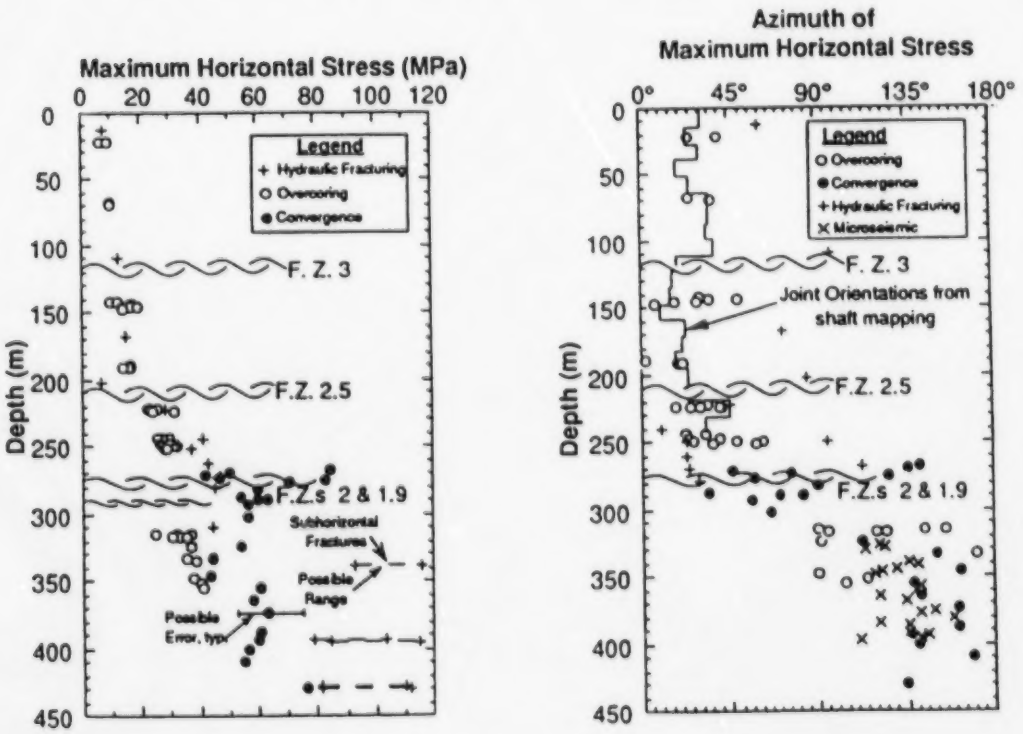

Figure 2.2 Variation of maximum horizontal stress orientation and magnitude with depth at URL site [1]

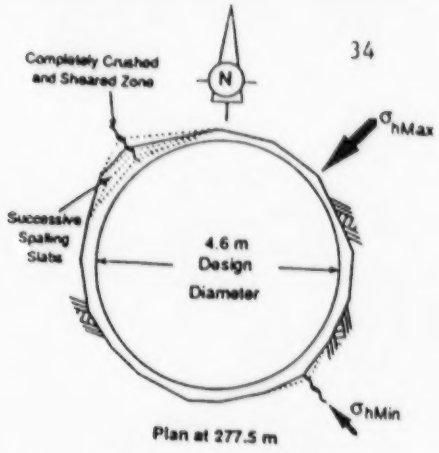

Figure 2.3 Formation of V-shaped notch during URL shaft failure at 277.5-m depth after [1].

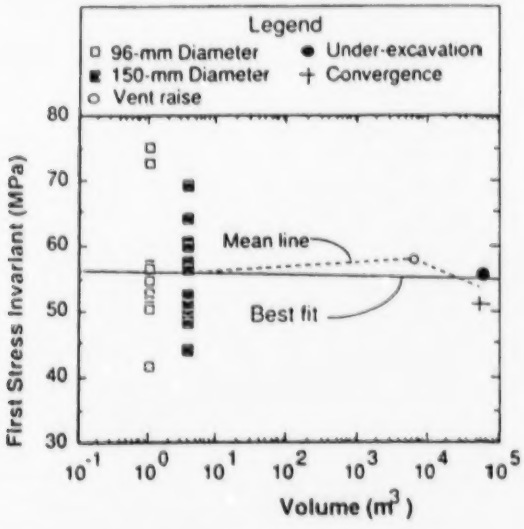

Figure 2.4 Scale effects of in situ stress after [1].

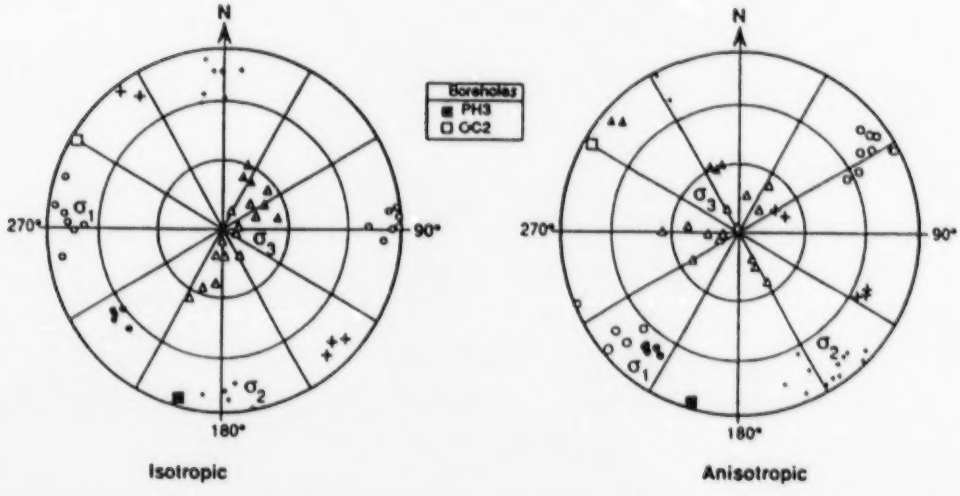

Figure 2.5 Comparison of principal stress orientations obtained from overcoring in boreholes PH3 and OC2 using closed-form solutions with linear elastic isotropic properties (left) and closed-form solutions with transverse anisotropic linear elastic properties (right) after [1].

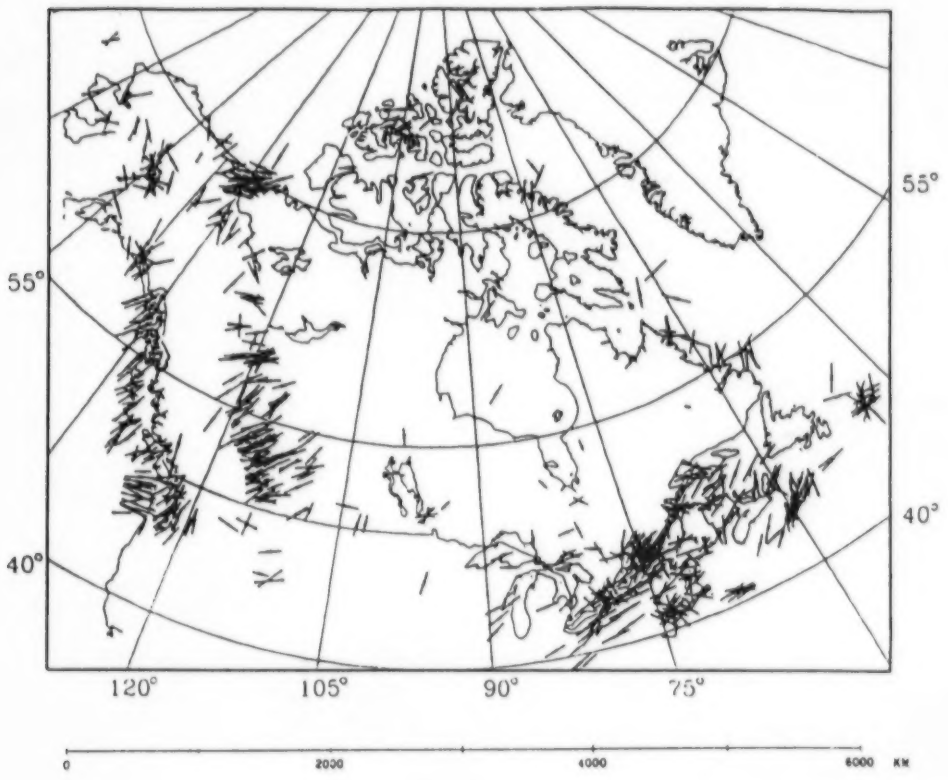

Figure 3.1 Maximum horizontal stress directions in Canada [6]

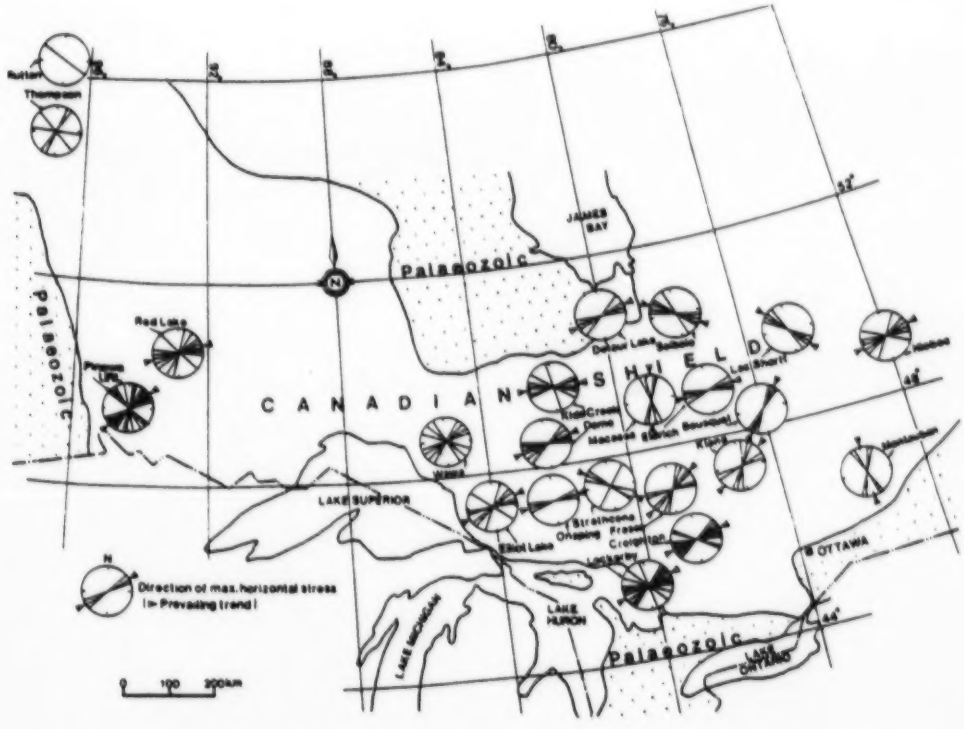

Figure 3.2 Maximum horizontal stress directions from overcoring in the Canadian shield [13]

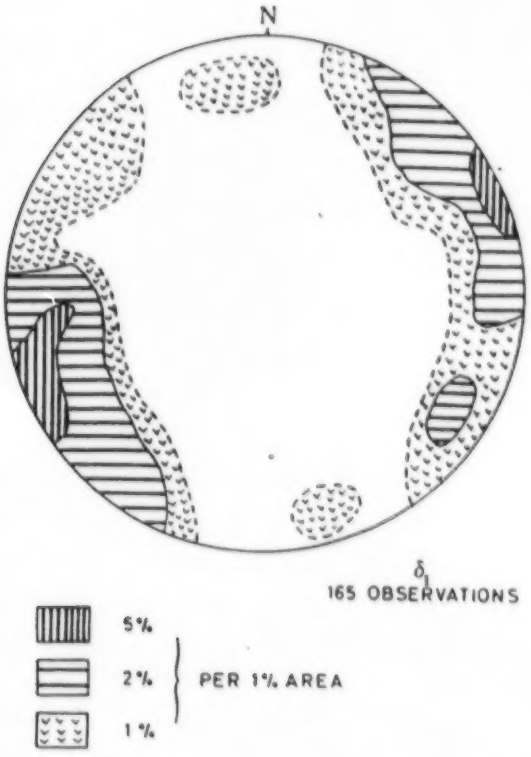

Figure 3.3 Orientation of σ_1

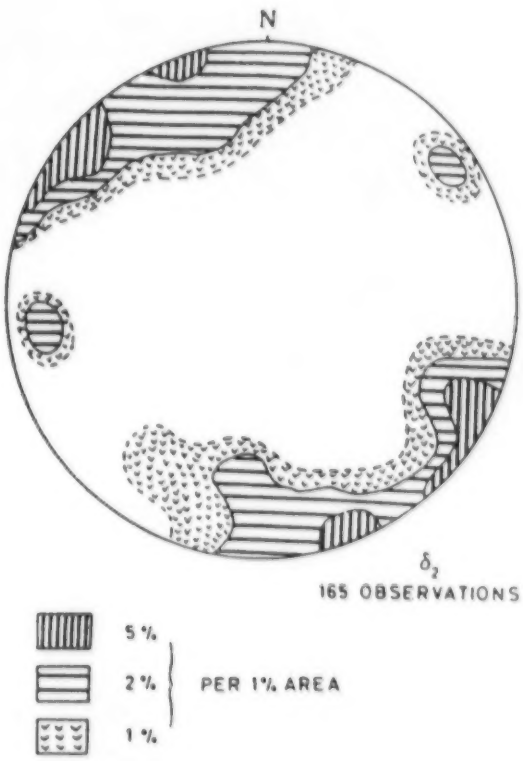

Figure 3.4 Orientation of σ_2

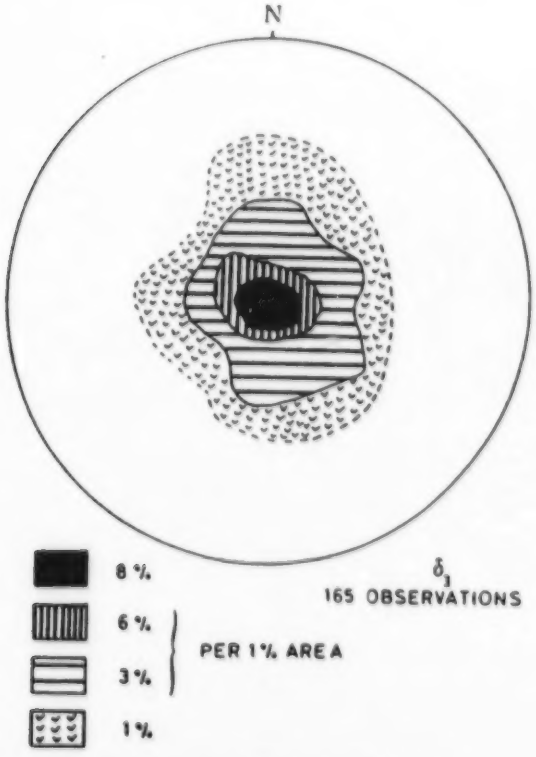

Figure 3.5 Orientation of σ_3

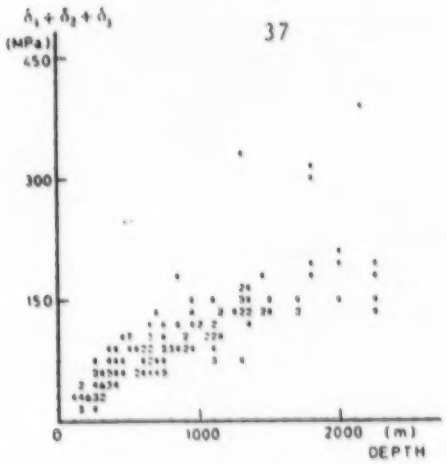

Figure 3.6 Sum of principal stresses with depth

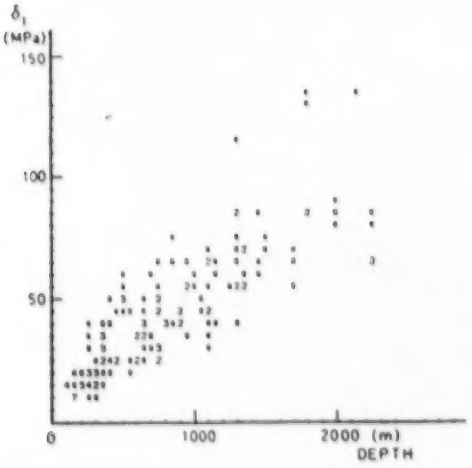

Figure 3.7 Maximum principal compressive stresses with depth

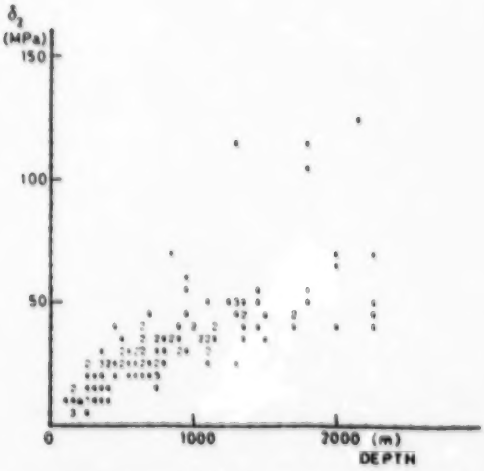

Figure 3.8 Intermediate principal compressive stresses with depth

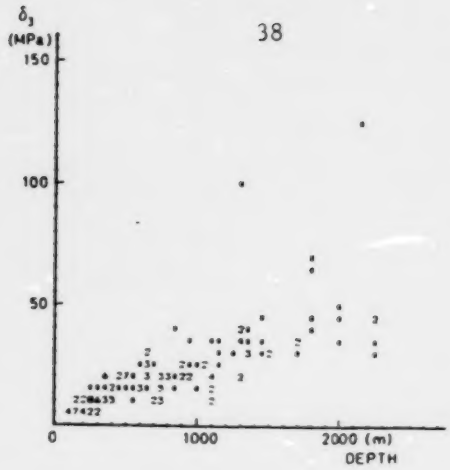

Figure 3.9 Minimum principal compressive stresses with depth

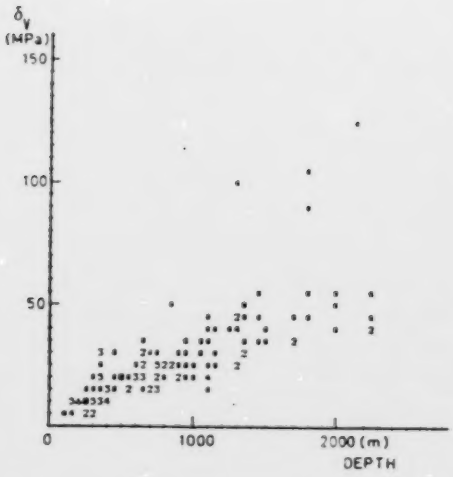

Figure 3.10 Change of vertical stress with depth

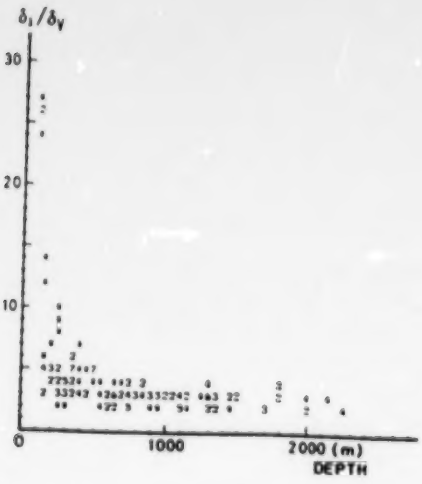

Figure 3.11 Maximum stress/vertical stress with depth

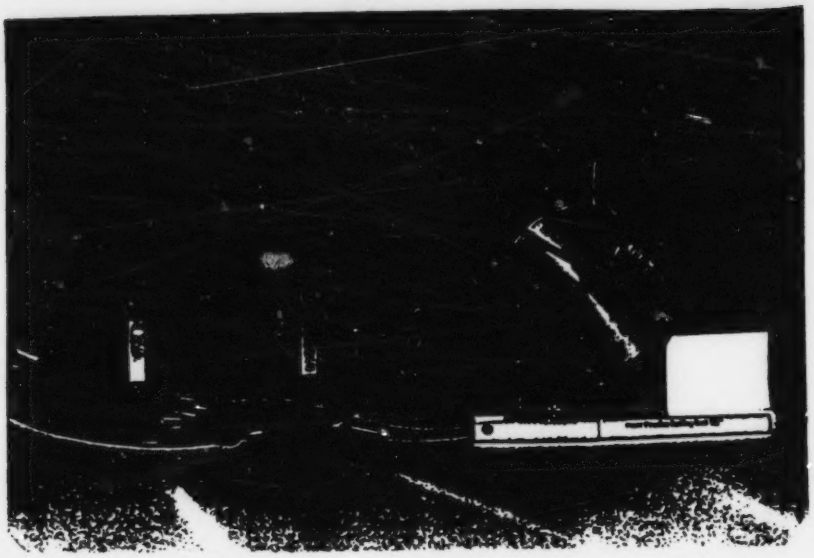

Figure 4.1 CANMET single axis strain monitor with hand held readout unit.

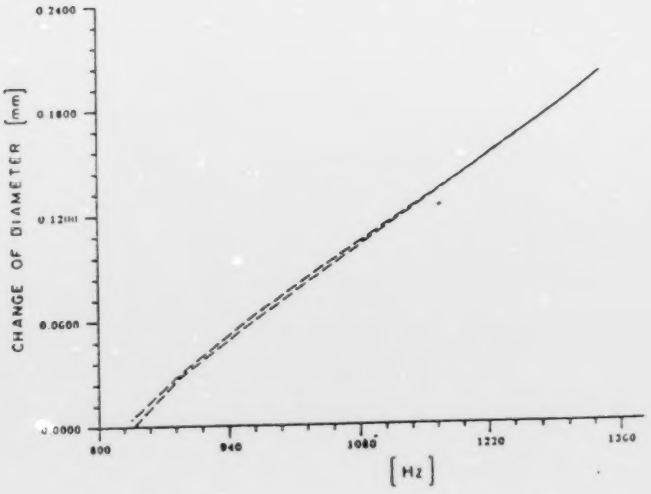

Figure 4.2 Calibration curve for CANMET strain monitor

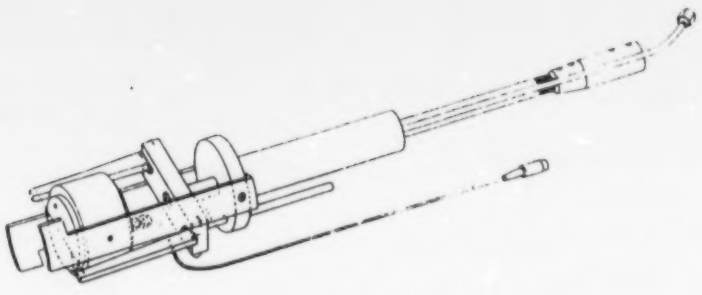

Figure 4.3 Installation tool for strain monitor

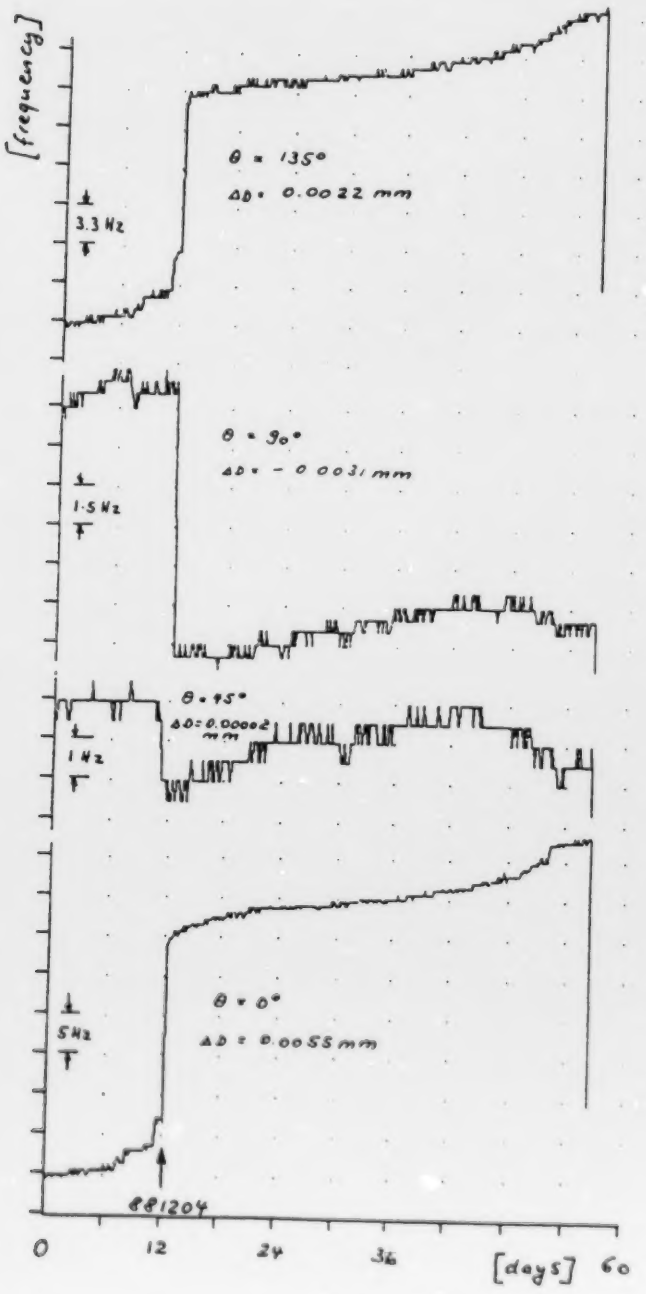

Figure 4.4 CANMET strain monitor response after production blast

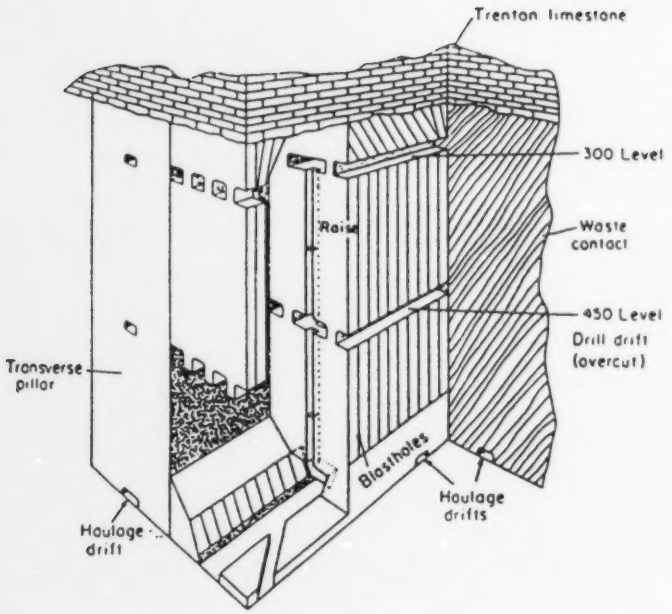

Figure 4.5 Blasthole open stope at Niobec Mine, Québec.

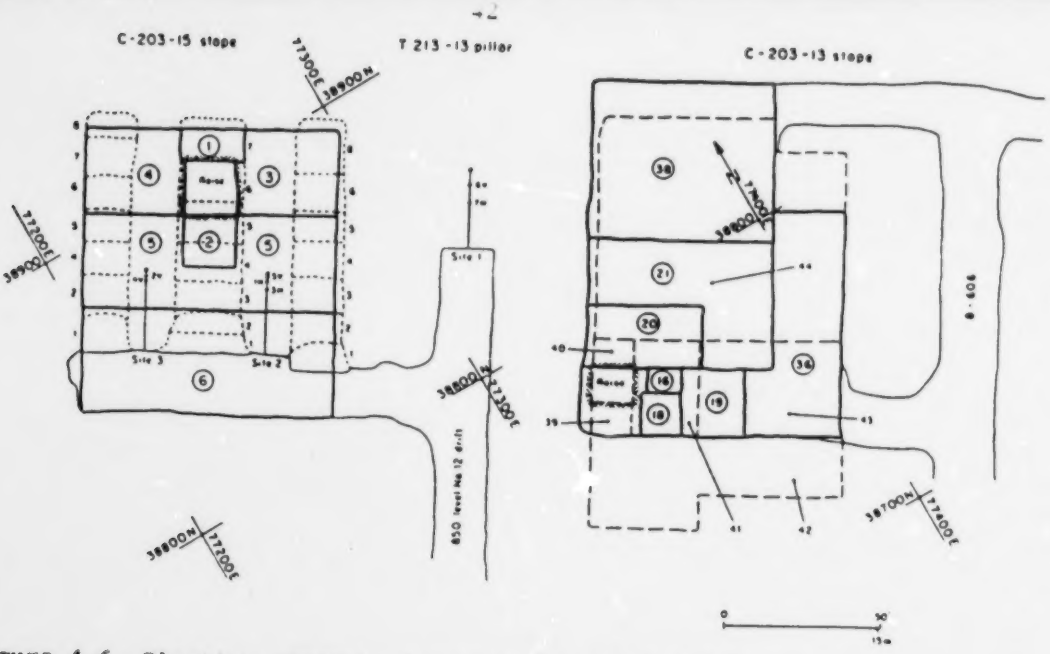

Figure 4.6 Blasting sequence for C-203-15 and C-203-13 stopes on 850 Level.

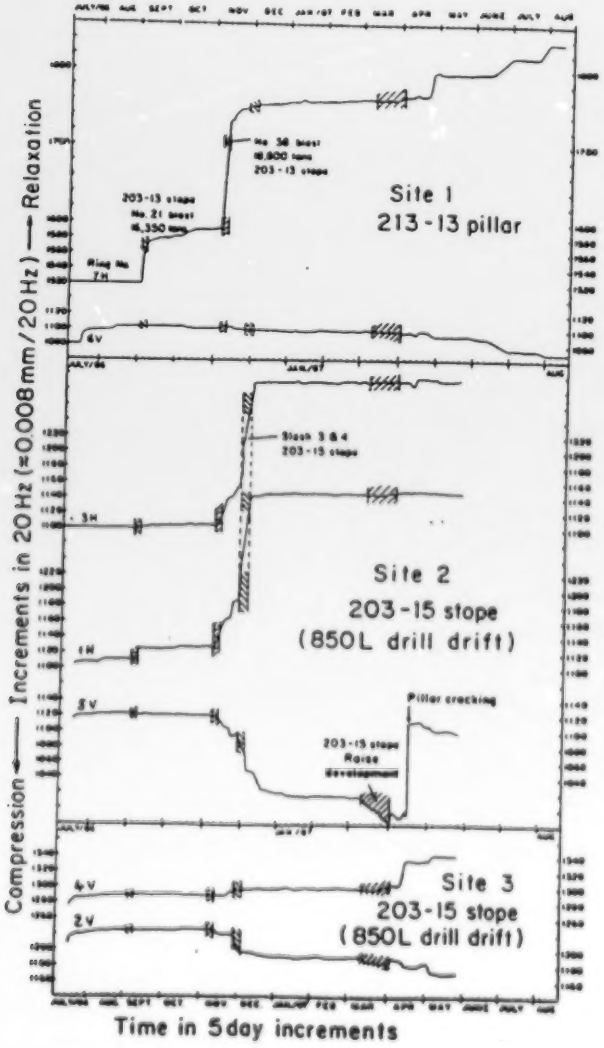

Figure 4.7 Response of vibrating wire sensors to blasting activity

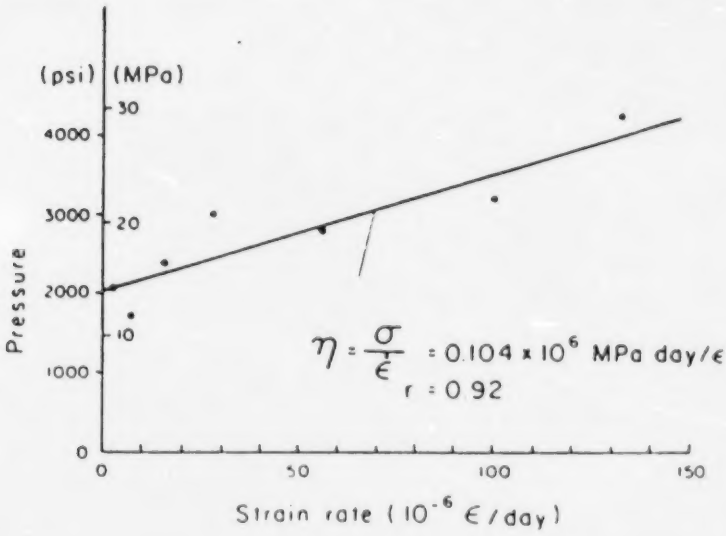

Figure 4.8 Viscosity constant from field data for Saskatchewan potash

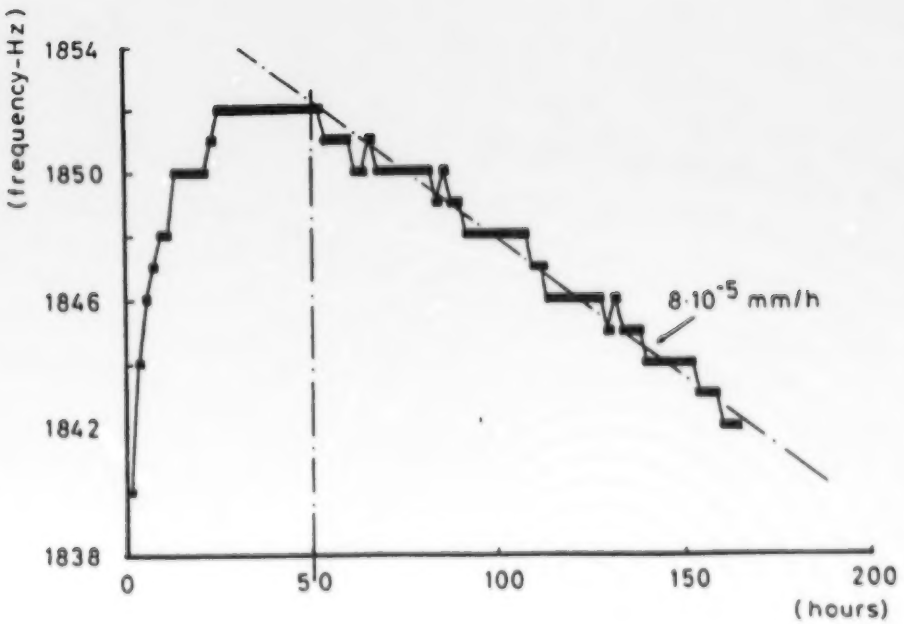

Figure 4.9 CANMET borehole tool establishes deformation rate in potash mine in New Brunswick